Nebot E., Durrant-Whyte H., "Initial Calibration and Alignment of Low Cost Inertial Navigation Units for Land Vehicle Applications", Journal of Robotics Systems, Vol. 16, No. 2, February 1999, pp. 81-92.

Initial calibration and alignment of Low cost Inertial Navigation Units for land vehicle applications

Eduardo Nebot, Hugh Durrant-Whyte.

Department of Mechanical and Mechatronic Engineering

University of Sydney, 2006, NSW, Australia.

nebot@mech.eng.usyd.edu.au

ph: 61-2-9351-2343

fax: 61-2-9351-7474

Published: Journal of Robotics Systems, Vol. 16, No. 2, February 1999, pp. 81-92.

Abstract

This work presents an efficient initial calibration and alignment algorithm for a six-degree of freedom inertial measurement unit (IMU) to be used in land vehicle applications. Error models for the gyros and accelerometers are presented with a study of their perturbation in trajectory prediction. A full inertial error model is also presented to determine the sensors needed for full observability of the different perturbation parameters. Finally, dead reckoning experimental results are presented based on the initial alignment and calibration parameters obtained with the algorithms presented. The results show that the algorithms proposed provide accurate position and velocity information for extended period of time using non-aided IMU.

Nebot E., Durrant-Whyte H., "Initial Calibration and Alignment of Low Cost Inertial Navigation Units for Land Vehicle Applications", Journal of Robotics Systems, Vol. 16, No. 2, February 1999, pp. 81-92.

1. Introduction

Vehicle automation has become an active research area with applications in mining, agriculture, construction and stevedoring. There are a number of publications considering the integration and commercialization of sensor suites for navigation systems [1-3]. To accomplish the reliability and integrity desired, these vehicles will almost certainly require the use of multiple sensors of varying types and algorithms to process the data available. The algorithms must provide fault detection and data fusion capabilities to make the best use of the information available. The sensors commonly used in these applications may be broken down into two broad categories, dead reckoning sensors, and external sensors [4]. While dead reckoning sensors tend to be very robust, they accumulate error with time. In practice they must be periodically reset using information from external sensors. External sensors provide absolute information, typically by making measurements of known landmarks.

Together these two sources of information span the complete frequency spectrum in a complimentary manner. As a general rule, absolute sensors provide low-frequency information and rate sensors provide high frequency information. A complete navigation algorithm will exploit this by using low-frequency sensor information to correct low-frequency drift error in high frequency sensors and by using high-frequency sensor information to decorrelate high-frequency noise from high frequency manoeuvres in low-frequency sensor information. The architecture that contemplates this combination of sensors is shown in figure **1** .

In these applications, a key to ultimate commercial success is the development of a navigation system whose performance is quantifiable, which can detect and recover from failures in individual sensor units and which can operate reliably and predictably in all operating conditions. To achieve this degree of system integrity the navigation system must have multiple navigation loops designed with sensors based on different physical principles to avoid similar faults. Most dead reckoning systems are based on encoders and tachometers. As demonstrated in [3], in some applications the information provided by these sensors can be in fault due of the predominant slip in the vehicle maneuver. In such cases, inertial sensors are the ideal candidates to provide the high frequency information to predict the position and orientation of the vehicle.

Inertial sensors make measurements of the internal state of the vehicle. A major advantage of inertial sensors is that they are non-radiating and non-jammable and may be packaged and sealed from the environment. Historically, INS have been used in aerospace vehicles [5], military applications, such as ships, submarines, missiles [6], and to a much lesser extent, in land vehicles applications [7]. Only few years ago the application of inertial sensing was limited to high performance-high cost aerospace and military applications [10]. However, several contributions in non-military applications have recently been published making use of low cost inertial systems, [11], [9], [8], [16].

Typical inertial sensors are accelerometers and gyroscopes. Accelerometers measure acceleration with respect to an inertial frame. These accelerations include gravitational and rotational accelerations as well as linear acceleration. Gyroscopes measure rate of rotation independent of coordinate frame. The most common application of inertial sensors is in the use of heading gyros. The integration of the gyro rate information provides the orientation of the vehicle.

Another application of inertial sensors is the use of accelerometers to measure the attitude of the vehicle. The tilt of a platform can be evaluated with two orthogonal accelerometers knowing the gravity magnitude in the region of operation. There are tilt sensors that provide very accurate information while the vehicle is stationary. When the vehicle is moving the accelerometers will also measure translational acceleration making the tilt information less accurate. Although this problem can be addressed for some very low speed applications [12], tilts sensors are not recommended for in-fligh alignment and calibration.

A full inertial navigation system (INS) consists of at least three (triaxial) accelerometers and three orthogonal gyroscopes providing acceleration in three dimensions and rotation rates about three axes. Theoretically, single and double integration of the gyro and accelerometer outputs will provide velocity and position information. In practice when working with standard IMU units, the non-linearity and noise present in the sensors make the trajectory prediction valid for short periods of time. The predicted trajectory will be a function of the initial calibration and alignment of the platform. By calibration it is mean the determination of biases on the accelerometers and gyros. The alignment process consists of determining the initial orientation of the platform. This is very important since the dead-reckoning algorithm uses this initial orientation to update the attitude information. The orientation of the platform is essential to obtain acceleration in the navigation frame and then to evaluate the single and double integration for velocity and position determination.

In order to work with an INS system for long periods of time it is necessary to reset the unit while the vehicle is stationary or use additional information to perform in-fligh alignment and calibration. The Global Positioning System (GPS) is frequently used in outdoor application in combination with IMU [16], [System, Kluwer, Dardrecht, 1998.

[14]. The IMU unit provides high frequency information in order to generate position estimates between GPS position and velocity fixes. Furthermore the data provided by the GPS sensor may be faulty or may not be available for extended periods of time. During these periods the IMU will have to provide the navigation information.

In-fligh calibration and alignment for land vehicles has proven to be very difficult, making the stationary algorithm of fundamental importance. In many applications, such as underground mining, it is very difficult to obtain external information with the quality required to calibrate and align the inertial unit while the vehicle is moving. In these applications the machines undergo frequently stops for loading and unloading operation making the stationary calibration and alignment algorithms absolutely essential for the INS system.

The algorithm presented in this work makes use of pendulum gyros to obtain initial orientation and biases of a full six-degree of freedom IMU. Experimental results are presented using a standard IMU equipped with three quartz accelerometers, three vibrating-beam gyros and two pendulum gyros. The information is sampled in the unit with 16 bit presition and transmitted serially to the navigation computer. The position prediction is compared to the "true" position obtained with an DGPS unit. The DGPS errors in position determination are of the order of 37 cm. CEP, or 95 cm. 95% of the time. An additional feature of this receiver is that it can provide position information at a rate of up to 20 Hz., making this unit very appropriate to test the algorithms designed.

This paper is divided into five main sections. Section 2 introduced the problematic involved with inertial sensors, presenting appropriate error models to characterize their faults. The algorithm to track orientation and predict position and velocities are also presented. Section 3 presents the calibration and alignment algorithms. Finally section 4 presents the experimental results with the conclusion given in Section 5.

2. Inertial Systems

Inertial Navigation Sensors

A full inertial navigation system (INS) consists of at least three (triaxial) accelerometers and three orthogonal gyroscopes to provide measurements of acceleration in three dimensions and rotation rates about three axes. An INS system assembled from low cost solid-state components is almost always constructed in a "strap-down" configuration. This term means that all of the gyros and accelerometers are fixed to a common chassis and are not actively controlled on gimbals to align themselves in a pre-specified direction. This design has the advantage of eliminating all moving parts. The strap-down construction, however, means that substantially more complex software is required to compute and distinguish true linear acceleration from angular acceleration and body roll or pitch with respect to gravity. Once true linear acceleration has been determined, vehicle position may be obtained, in principle, by double integration of the acceleration. Vehicle orientation and attitude may also, in principle, be determined by integration of the rotation rates of the gyros. In practice this integration leads to unbounded growth in position errors with time due to the noise associated with the measurement and the non-linearity of the sensors. In this section we present the main sources of errors of inertial sensors and an estimation of their influence in the trajectory error determination.

Accelerometer and Gyro errors

There are many different types of accelerometers and gyroscopes [15]. The accelerometers measure the absolute acceleration with respect to an inertial frame. We are interested in the translational acceleration, hence the algorithms used must compensate for all other accelerations. For practical purposes it can be considered that gravity is the only unwanted acceleration present. Figure 2 shows the acceleration obtained during a standard vehicle run at less than 60 km/h. It can be seen that the magnitude of the acceleration measured is smaller that 0.3 g. This implies that the orientation of the accelerometer has to be known with very good accuracy to compensate for gravity without introducing errors comparable to the actual translation acceleration.

The orientation of the accelerometer can be tracked with gyroscopes. These sensors provide an output proportional to the rotation velocity contaminated by noise and drift. For short periods of time the drift can be approximated by a constant bias. The actual orientation is obtained using the following equation:

$$\theta_m = \int \dot{\theta} + b + v \; dt \quad = \quad \theta + bt \; + \int v \, dt \tag{1}$$

It can be seen that this integration will return the rotation angle with two additional undesired terms. A random walk due to the noise υ and another term that grows with time proportional to the gyro bias *b*.

The random walk will generate an error that is proportional to the standard deviation of the noise and the square root of time. Figure 3 presents the integration of 3 minutes of data obtained from a stationary gyro. It can be seen that although maximum bounds can be predicted each run has a different final value.

Another important source of error is gyro drift. Figure **4** presents the case of a constant drift "b" in the gyro measuring the z rotation. This error will translate in an incorrect orientation evaluation of the x and y accelerometers coupling the acceleration x into the y axis. A constant acceleration ax in the x direction will introduce errors in the acceleration, velocity and position in the y direction. Assuming the small angle approximation, these error can be evaluated:

$$e_{ay} = ax\,b\,t\,, \qquad e_{vy} = \frac{1}{2}ax\,b\,t^2\,, \qquad e_{py} = \frac{1}{6}ax\,b\,t^3 \tag{2}$$

It can be appreciated that a constant gyro bias will introduce errors in position determination proportional to t^3.

Figure 5 presents the gyro and accelerometer drift of the IMU during a period of 6 hours of operation. It can be appreciated that there is a considerable bias variation that can not, in general, be predicted due to the internal hardware compensations implemented in the individual sensors. The bias expected from a standard low cost, good quality gyro is in the order of 10 degrees / hour. Without calibration the expected bias could introduce an error of approximately 142 meters after only 2 minutes of operation due to the incorrect compensation of gravity.

The bias in the accelerometer will increase the error in position and is proportional to the square of time, as shown in the following equation

$$e_{vx} = b\,t\,, \qquad e_{px} = \frac{b\,t^2}{2} \tag{3}$$

As can be seen from the previous equations, biases in accelerometers and gyros must be determined before attempting to evaluate inertial attitude, position and velocities. Bias identification is usually performed by a calibration algorithm during the initialization stage.

Coordinate Systems and Transformations

The navigation algorithm is designed in a local geographic frame n, with axes $^{n}\{N, E, D\}$, (North, East and Down). It is necessary to determine the transformation from this frame to other frames since the various INS sensors and the GPS system provide information in different coordinate frames. Figure **6** shows the various coordinate frames involved in this project.

The GPS system provides information in the Earth frame e, with axes $^{e}\{X, Y, Z\}$. These axes are fixed to the Earth so that the X and Y axes rotate around the Z axis with the Earth's rotational velocity Ω.

The coordinate transformations from earth frame to the local navigation frame are presented in [13].

The inertial measurement unit is mounted on the vehicle constituting a new frame. This is called the body frame "b'', and has axes $^{b}\{R, P, Y\}$, (Roll, Pitch and Yaw). This frame will be in constant rotation with respect to the "n" (navigation) frame. The velocity of this rotation is measured by three near-orthogonal gyros. The transformation matrix C_b^n that relates the coordinates frames "b" and "n" can be obtained with the following integration:

$$\dot{C}_b^n = \Omega_{bn} C_b^n \qquad \Omega_{bn} = \begin{bmatrix} 0 & -\omega_Y & \omega_P \\ \omega_Y & 0 & -\omega_R \\ -\omega_P & \omega_R & 0 \end{bmatrix} \tag{4}$$

where Ω_{bn} is the antisymetric velocity matrix and $\omega_{R,Y,P}$ are the roll, yaw and pitch rotation velocities measured by the gyros in the body frame. In real time applications the integration can be implemented with the following approximation

$$C_b^n(k+1) = C_b^n(I + \Delta\theta)\,, with\ \ \Delta\theta = \begin{bmatrix} 0 & -\Delta\theta_Y & \Delta\theta_P \\ \Delta\theta_Y & 0 & -\Delta\theta_R \\ -\Delta\theta_P & \Delta\theta_R & 0 \end{bmatrix},\ I = \begin{bmatrix} 1 & 0 & 0 \\ 0 & 1 & 0 \\ 0 & 0 & 1 \end{bmatrix} \tag{5}$$

where *(I+Δθ)* is the small angle direction cosine matrix relating the frame at time k and the rotating frame at time k+1. This approximation is valid for small angles, which constrains the minimum sampling time of the gyros such that the transformation matrix may be obtained with reasonable accuracy. This sampling time will be a function of the severity of maneuvers expected from the vehicle. In this application the maximum rotation velocity expected is approximately 25 degrees/sec. When sampling at 100 Hz the maximum angle variation will be less than 0.25 degree. For applications where the small angle approximation can not be satisfied then additional terms needs to be considered in equation (5) or use a different method to update the transformation matrix, such as quaternions [17].

INS error model.

The dynamics of the Earth surface frame navigator can be described by the following set of equations:

$$\begin{aligned} \dot{R}^n &= V^n \\ \dot{V} &= C_b^n A_{bn}^b + g^n \\ \dot{C}_b^n &= \Omega_{bn}^n C_b^n \end{aligned} \qquad (6)$$

Where R,V, g^n are position, velocity and the gravity vector in the navigation frame n, A_{bn}^b is the acceleration vector in the body frame b, C_b^n is the transformation matrix from body frame b to navigation frame n and Ω_{bn}^n is the anti-symetric matrix given in equation 4.

The simplified system error model can be written in terms of errors in position R, velocity V and the misalignment angles Φ:

$$\begin{bmatrix} \dot{r} \\ \dot{v} \\ \dot{\phi} \end{bmatrix} = \begin{bmatrix} 0 & I & 0 \\ 0 & 0 & a_n \\ 0 & 0 & 0 \end{bmatrix} \begin{bmatrix} r \\ v \\ \phi \end{bmatrix} + \begin{bmatrix} 0 \\ C_b^n e_a \\ C_b^n e_g \end{bmatrix}, \quad \dot{x} = F_g x + G w \qquad (7)$$

The INS platform is built with low cost gyros and accelerometers. In equation 7, e_a and e_g are the error vectors in the body frame due to accelerometers and gyros errors. The matrix C_b^n transforms these values into the navigation coordinate frame.

The gyro error model proposed consist of a first order Markov process with correlation time τ plus white noise ν:

$$\dot{\theta} = -(1/\tau)\theta + \nu_g, \quad E[\nu_g] = 0, \quad E[\nu_g \nu_g{}^T] = R_g \qquad (8)$$

The matrix contemplating the time constant for the three gyros is T_g

$$T_g = \begin{bmatrix} -1/\tau_x & 0 & 0 \\ 0 & -1/\tau_y & 0 \\ 0 & 0 & -1/\tau_z \end{bmatrix} \qquad (9)$$

The error model for the accelerometers consists of a random constant component plus white noise:

$$a = \nu_a \qquad E[\nu_a] = 0, \quad E[\nu_a \nu_a{}^T] = R_a \qquad (10)$$

The matrix for the accelerometer errors is T_a

$$T_a = [0_{3x3}] \qquad (11)$$

Finally the complete state error model has the following form:

$$\dot{x} = Fx + Gw \qquad (12)$$

with

$$F = \begin{bmatrix} & & & 0 & 0 \\ & F_g & & C_b^n & 0 \\ & & & 0 & C_b^n \\ 0 & 0 & 0 & T_a & 0 \\ 0 & 0 & 0 & 0 & T_g \end{bmatrix}, \quad G = \begin{bmatrix} 0 & 0 & 0 & 0 & 0 \\ 0 & C_b^n & 0 & 0 & 0 \\ 0 & 0 & C_b^n & 0 & 0 \\ 0 & 0 & 0 & I & 0 \\ 0 & 0 & 0 & 0 & I \end{bmatrix}, \quad x = \begin{bmatrix} r \\ v \\ \phi \\ b_g \\ b_a \end{bmatrix}$$

where *r,v* and ϕ are the errors in position, velocity and angle misalignments, and b_g and b_a are the bias errors in the gyros and accelerometers in the body frame. For initial alignment and calibration purposes the model is simplified neglecting the error in position "*r*". The Transformation matrix C_b^n is included in the model to reference all the biases to the navigation frame.

Observations

Initial alignment and calibration is usually performed while the vehicle is stationary. The three observations of zero velocities can be used to identify the unknown parameters. The model that relates the observations to the states can be written in the following form

$$z = Hx + D\upsilon \tag{13}$$

with

$$H = \begin{bmatrix} I_{3*3} & 0_{3*9} \end{bmatrix} \tag{14}$$

By making an observability analysis it can be proved that the system is not observable while the platform is not moving. It will not be possible to identify misalignment and biases in the accelerometers from observation taken at only one position. This is due to the fact that zero vector velocity does not provide heading information. When the platform moves, the vector velocity provides three dimensional heading information that can be used to calibrate the IMU. In some military applications it is possible to plan particular maneuvers for calibration and alignment purposes. For land vehicle applications in general it will not be acceptable to require a trajectory to generate enough information to calibrate and align the unit.

There are commercially available tilt units with the precision required to align and calibrate a low cost INS system. In this particular implementation the bank and elevation angles are provided by two stable pendulum gyros. Although heading is also required for complete alignment, it's accuracy is not as critical as the vertical orientation determination since it will introduce trajectory errors that are independent of time. This is due to the fact that the gravity vector is independent of the heading orientation.

The tilt and heading information will modify the observation matrix H as shown below

$$H = \begin{bmatrix} I_{3*3} & 0 & 0 \\ 0 & I_{3*3} & 0 \end{bmatrix} \tag{15}$$

The new set of measurements makes the system fully observable while stationary.

3. Calibration and Alignment algorithm

The initial orientation of the platform is needed to initialize the INS. This section presents a method to obtain the initial transformation matrix C_b^n and the biases in the accelerometers and gyros. The unknowns are the gyro and accelerometer biases and the orientation of the platform, that is the inclination of the x-y plane and its orientation with respect to north. The inclination (tilt) of the platform can be obtained, in principle, from the accelerometers x and y, but the unknown biases prevent the accurate determination of the tilt.

The Direction Cosine matrix C_b^n can be defined considering three successive rotation of angles θ, β, γ around the x, y and z axis respectively and in that order. The order of the rotation is of fundamental importance since these operations are not commutative. The transformation matrix is described in equation 16

$$\begin{bmatrix} a^{nx} \\ a^{ny} \\ a^{nz} \end{bmatrix} = \begin{bmatrix} \cos\beta\cos\gamma & -\cos\theta\sin\gamma + \sin\theta\sin\beta\cos\gamma & \sin\gamma\sin\theta + \cos\theta\sin\beta\cos\gamma \\ +\cos\beta\sin\gamma & \cos\theta\cos\gamma + \sin\theta\sin\beta\sin\gamma & -\sin\theta\cos\gamma + \cos\theta\sin\beta\sin\gamma \\ -\sin\beta & +\sin\theta\cos\beta & \cos\theta\cos\beta \end{bmatrix} \begin{bmatrix} a^{bx} \\ a^{by} \\ a^{bz} \end{bmatrix} \quad (16)$$

This matrix relates the acceleration in the body and local navigation frame, that is

$$a^n = C_b^n a^b \quad (17)$$

being a^b the raw acceleration measured by the accelerometers in the body frame and a^n the transformed acceleration in the navigation frame (N, E, D).

The bias presents in the measured acceleration a^b can be estimated with the external tilt information. The pendulum gyros return angular information following the standard gyro convention. They measure bank and elevation with respect to plane tangential to the earth. This plane is coincident with the local navigation frame. The acceleration measured in x, y and z are then compensated according to the individual projection of the gravity vector in each axis:

$$\begin{aligned} a_{bias}^{bx} &= a_{meas}^{bx} - \sin(elevation) \\ a_{bias}^{by} &= a_{meas}^{by} + \sin(bank) \\ a_{bias}^{bz} &= a_{meas}^{bz} - (1 - \cos(elevation) * \cos(bank)) \end{aligned} \quad (18)$$

During initial alignment, the vehicle is assumed to be stationary. The velocities and accelerations of the platform can be considered zero except for gravity. The acceleration measured in the navigation frame is:

$$a^n = C_b^n a^b \; with \;\; a^n = \begin{bmatrix} 0 & 0 & g \end{bmatrix}^T \tag{19}$$

After removing the bias, the measured acceleration in the body frame can be evaluated using:

$$a^b = C_n^b a^n \;\; with \;\; C_n^b = \left[C_b^n\right]^{-1} = \left[C_b^n\right]^T \tag{20}$$

Since the transformation matrix C is orthogonal, the inverse is equal to the transpose, then the acceleration in the body frame are:

$$\begin{bmatrix} a^{bx} \\ a^{by} \\ a^{bz} \end{bmatrix} = \begin{bmatrix} \cos\beta\cos\gamma & \cos\beta\sin\gamma & -\sin\beta \\ -\cos\theta\sin\gamma + \sin\theta\sin\beta\cos\gamma & \cos\theta\cos\gamma + \sin\theta\sin\beta\sin\gamma & \sin\theta\cos\beta \\ \sin\gamma\sin\theta + \cos\theta\sin\beta\cos\gamma & -\sin\theta\cos\gamma + \cos\theta\sin\beta\sin\gamma & \cos\theta\cos\beta \end{bmatrix} \begin{bmatrix} 0 \\ 0 \\ g \end{bmatrix} \tag{21}$$

With the tilt information (bank and elevation angles), the value of the measured body acceleration can be predicted after compensating for the biases. This information can be obtained from the third column of the transformation matrix. The following equations can then used to solve for the Euler angles θ and β

$$\begin{aligned} \sin\beta &= \sin(elevation) \\ \sin\theta\cos\beta &= \sin(bank) \end{aligned} \tag{22}$$

From equation 22 the Euler angles θ and β can be evaluated using

$$\begin{aligned} \beta &= elevation \\ \theta &= \sin^{-1}\left(\frac{\sin(bank)}{\cos(-elevation)}\right) \end{aligned} \tag{23}$$

The remaining Euler angle γ can be evaluated with the external heading information:

$$\gamma = heading \;\; angle \tag{24}$$

Finally the transformation matrix C_b^n can be evaluated with equation 16 using the Euler angles θ, β and γ.

4. Implementation and Experimental Results.

A block diagram describing the algorithms involved to obtain inertial indicated position and orientation is shown in Figure 7.

The IMU provides raw gyro and accelerometer data. The additional tilt and heading sensors are used for calibration and alignment purposes to estimate the biases and the initial orientation of the unit in the navigation frame ($C_b^n(0)$). Then the system tracks the platform orientation using the gyros information to update the transformation matrix ($C_b^n(k)$). Finally the accelerations in the navigation frame are obtained to perform single and double integration to obtain velocities and position in the navigation frame.

For this experiment the IMU, GPS and the data acquisition system were installed in a Holden Ute vehicle shown in Figure 8 . The algorithms were implemented using a transputer based system.

The vehicle was driven for 3 minutes in a trajectory of approximately 1 km. long. Initially the vehicle was at rest, with the engine on, for a period of approximately 15 seconds. This stationary data was used for calibration and alignment purposes. Figure **2** shows the raw acceleration in the x direction. It can be seen that the accelerations measured are in the range of +/- 0.3 g. This makes the alignment problem very important since small errors in attitude determination will introduce large comparative errors due to the erroneous compensation for the gravity vector.

Figure **9** and 10 show the acceleration and pendulum gyro measurements used for calibration. A 15-second average was used in order to filter the engine vibration information. It can be clearly seen that the acceleration information is biased since both the x and y acceleration have different signs while the pendulum gyros are indicating that roll and pitch have negative signs.

The calibration and alignment algorithm was used to estimate the biases and to obtain the initial transformation matrix. The raw accelerations were compensated and the initial 40 seconds are shown in Figure **11**. It can be clearly seen that the compensation is almost perfect since the acceleration in the x and y direction are zero while the vehicle is at rest. The compensated gyro information was then used to track the cosine matrix transformation with the approximation presented in equation 5. Equation 6 was integrated to obtain the acceleration, velocity and position in the navigation coordinate frame. Figure **12** and 13 present the velocity and position prediction compared with the true values measured with a DGPS unit. It can be seen the INS prediction, black, follows the true trajectory with small error for approximately 100 seconds. These results are very important since they show how the dead reckoning errors grow using the IMU without aiding information.

The 2-D trajectory is presented in figure **14**. An enhanced view of the first 160 meters is also shown in Figure 15. During this part of the run the DGPS system experienced some multipath errors that can easily be rejected with the additional INS information. For a more details of fault detection in GPS/INS system the reader is referred to [14]. Finally Figure **16** and 17 represent the history of the Euler angles information during the run. The yaw angle is changing 360 degrees per turn but roll and pitch have very small variations but high frequency components due to the roughness of the terrain. In land vehicle applications the errors in roll and pitch can be catastrophic since they are mainly responsible for the gravity vector compensation. The selection of the roll and pitch gyros should contemplate the terrain type since it will be responsible for the maximum rate measured by these gyros.

5. Conclusion

This works presented an efficient initial calibration and alignment algorithm to work with standard low cost Inertial Measurement Units. An observability analysis has been presented that has shown that the initial alignment is not possible when using low cost accelerometers. Additional tilt information is necessary to differentiate bias in the accelerometers from misalignment angles. The experimental results have shown that the initial calibration and alignment is accurate enough to allow navigation with IMU sensors for extended period of time with low dead reckoning errors. Future work will investigate in-flight calibration and alignment algorithms extending the error models of the INS system.

6. References

[1] Labonte F., J., Giraud L., and Polotski V., "Telerobotics issues in the operation of a LHD vehicle", Proc. of the Third Canadian Conference on Computer Applications in the Mineral Industry, 1995, pp 672-681

[2] Makela H., Lehtinen H, Rintanen K., Koskinen K., Navigation System for LHD machines", Intelligent Autonomous Vehicles 95. Finland, pp. 314-319, 1995.

[3] S. Scheding, G. Dissanayake, E. Nebot and H. Durrant-Whyte, "Slip Modeling and Aided Inertial Navigation of an LHD", IEEE Conference on Robotics and Automation, 1997, pp. 1904-1909.

[4] . Scheding, E. M. Nebot , M. Stevens and H. Durrant-Whyte, J. Roberts and P. Corke, Cunningham and B. Cook, "Experiments in Autonomous Underground Guidance", IEEE Conference on Robotic and Automation, 1997, pp. 1898-1903.

[5] Crocker E., Rabins L., "Applications of Kalman Filtering Techniques to strap-down system Initial Alignment", Theory and applications on Kalman Filters, Dr. E. M. Nebot by C. T. Leons, 1970, University of California,

[6] Rogers R., "Weapon IMU Transfer alignment using aircraft position from actual flight tests", - IEEE PLANS, Position Location and Navigation Symposium. 1996, pp. 328 – 333.

[7] Lapucha D., Schwarz K., Cannon M., Martell H., "The use of INS/GPS in a highway survey system", - IEEE PLANS, Position Location and Navigation Symposium. 1994, pp. 413-419.

[8] Jarvis, R. "All-terrain intelligent autonomous vehicle with sensor-fusion-based navigation capabilities", Control Engineering Practice. V 4 n 4 Apr 1996. p 481-486.

[9] Bonnifait Ph., Garcia G., "A Multisensor Localization Algorithm for Mobile robots and its real time experimental validation", Proc of the 1996 IEEE Robotics and Automation, Minneapolis, Minnesota., pp 1395-1400.

[10] Hyslop G., Geth D., Kraemer J., "GPS/INS integration on the standoff land attack missile (SLAM), IEEE PLANS, Position Location and Navigation Symposium. 1994. pp. 407-412

[11] Daum, P., Beyer J.,. Kohler T. Aided inertial land navigation system (ILANA) with a minimum set of inertial sensors Record - IEEE PLANS, Position Location and Navigation Symposium. 1994. Pp. 284-291

[12] Fuke Y., Krotkov E., "Dead reckoning for a lunar rover on uneven terrain", IEEE Int. Conf. Robotics and Automation, Minneapolis, Minnesota, 1996, pp. 411-416.

[13] Nebot E., "Sensor used for autonomous navigation", Chapter 7, pp 135-156, Advances in Intelligent Autonomous System, Kluwer, Dardrecht, 1998.

[14] Sukkarieh S., Nebot E., Durrant-Whyte H., "Achieving integrity in an GPS / INS navigation loop for land vehicle applications", IEEE International Conference of Robotic and Automation, Belgium, 1998, pp. 3437-3442.

[15] Lawrence A., "Modern Inertial Technology", 1993, Springer Verlag.

[16] Schonberg, T. Ojala, M. Suomela, J. Torpo, A. Halme, A. Positioning an autonomous off-road vehicle by using fused DGPS and inertial navigation International Journal of Systems Science. v 27 n 8 Aug 1996. p 745-752

[17] Titterton D. H., Weston J., "Strapdown Inertial Navigation Technology", IEE, UK, 1997. ISBN 0 86341 260 2.

Nebot E., Durrant-Whyte H., "Initial Calibration and Alignment of Low Cost Inertial Navigation Units for Land Vehicle Applications", Journal of Robotics Systems, Vol. 16, No. 2, February 1999, pp. 81-92.

Captions for figures

Figure 1 Single Loop Navigation Architecture

Figure 2. Raw Acceleration

Figure 3. Gyro random walk.

Figure 4. Gyro drift errors

Figure 5 Gyro and accelerometer drifts

Figure 6. Coordinate systems

Figure 7. Inertial Position and velocity determination

Figure 8 Experimental setup

Figure 9. Accelerometers output in body frame

Figure 10. Bank and Elevation output

Figure 11. Compensated acceleration (Navigation frame)

Figure 12. North velocity prediction

Figure 13. North position prediction

Figure 14. 2-D trajectory prediction

Figure 15. 2-D trajectory prediction

Figure 16. Euler Angles prediction (x,y,z)

Figure 17. Euler Angles prediction (x,y)

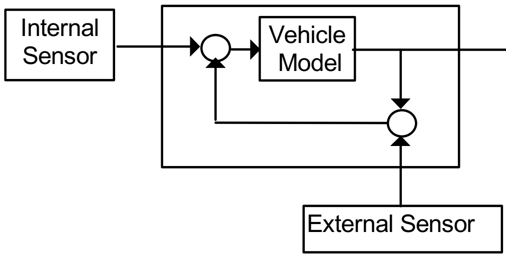

Figure 1 Single Loop Navigation Architecture

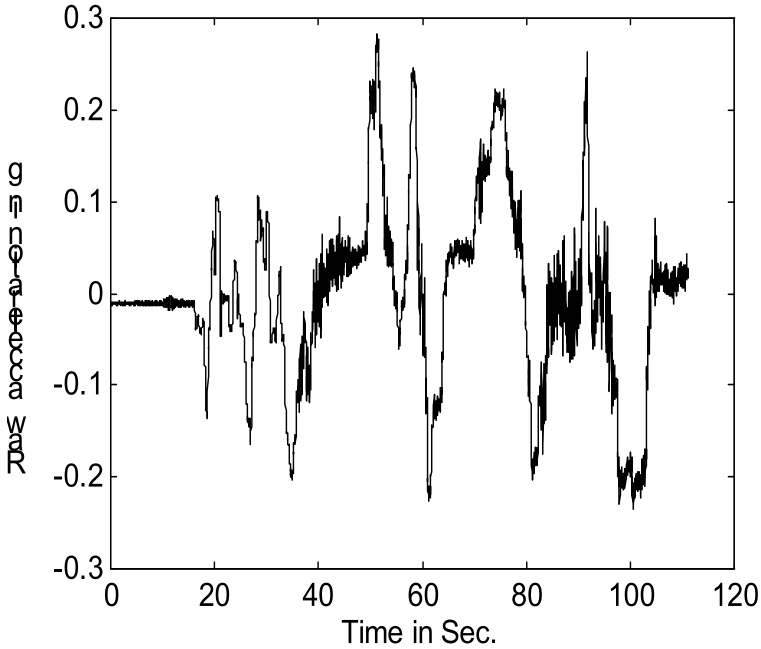

Figure 2. Raw Acceleration

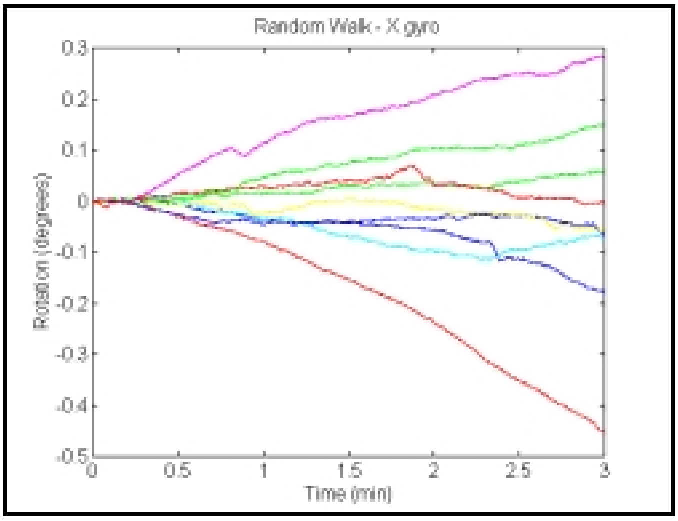

Figure 3. Gyro random walk.

Nebot E., Durrant-Whyte H., "Initial Calibration and Alignment of Low Cost Inertial Navigation Units for Land Vehicle Applications", Journal of Robotics Systems, Vol. 16, No. 2, February 1999, pp. 81-92.

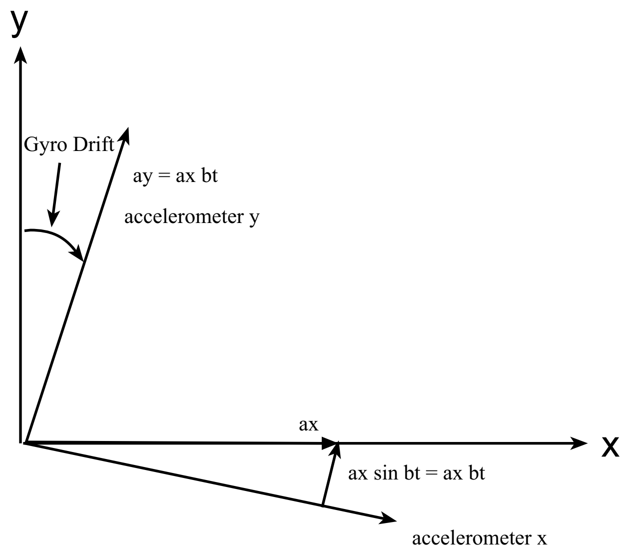

Figure 4. Gyro drift errors

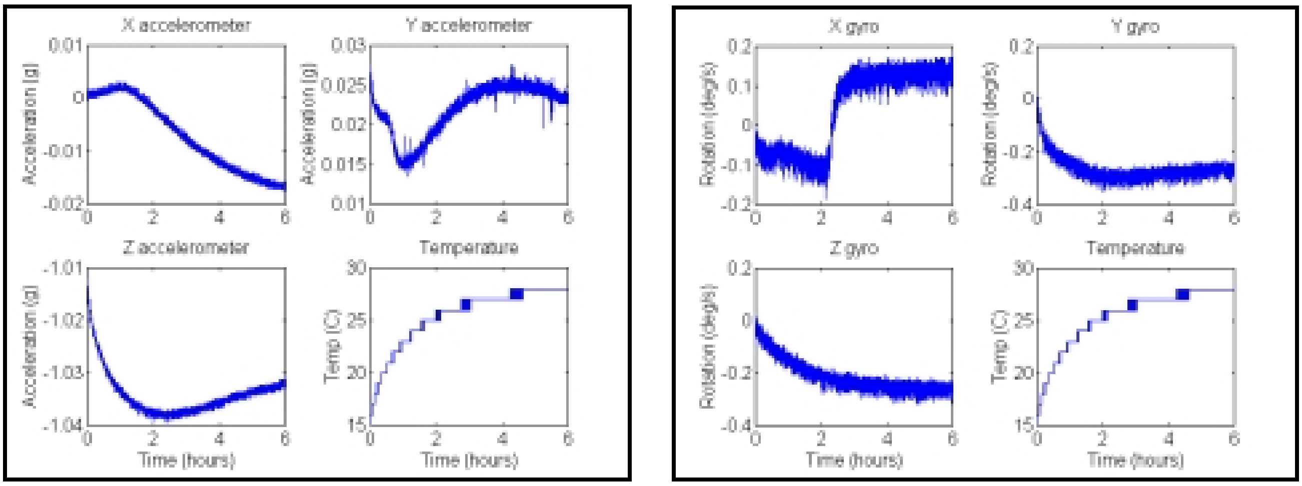

Figure 5 Gyro and accelerometer drifts

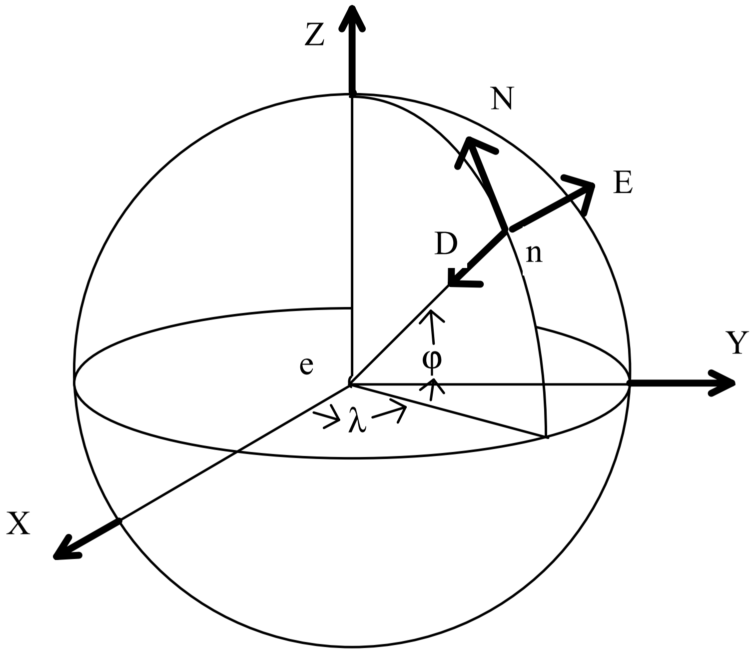

Figure 6. Coordinate systems

Nebot E., Durrant-Whyte H., "Initial Calibration and Alignment of Low Cost Inertial Navigation Units for Land Vehicle Applications", Journal of Robotics Systems, Vol. 16, No. 2, February 1999, pp. 81-92.

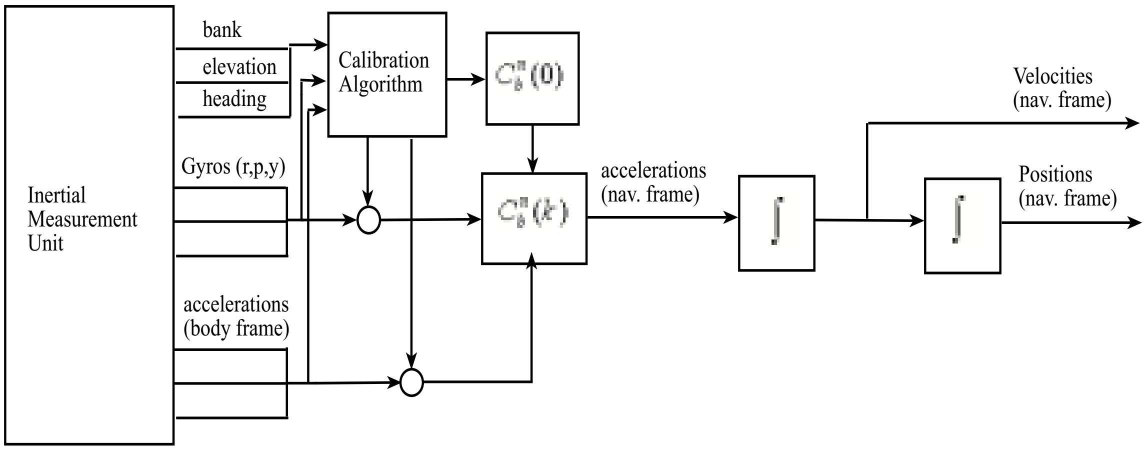

Figure 7. Inertial Position and velocity determination

Figure 8 Experimental setup

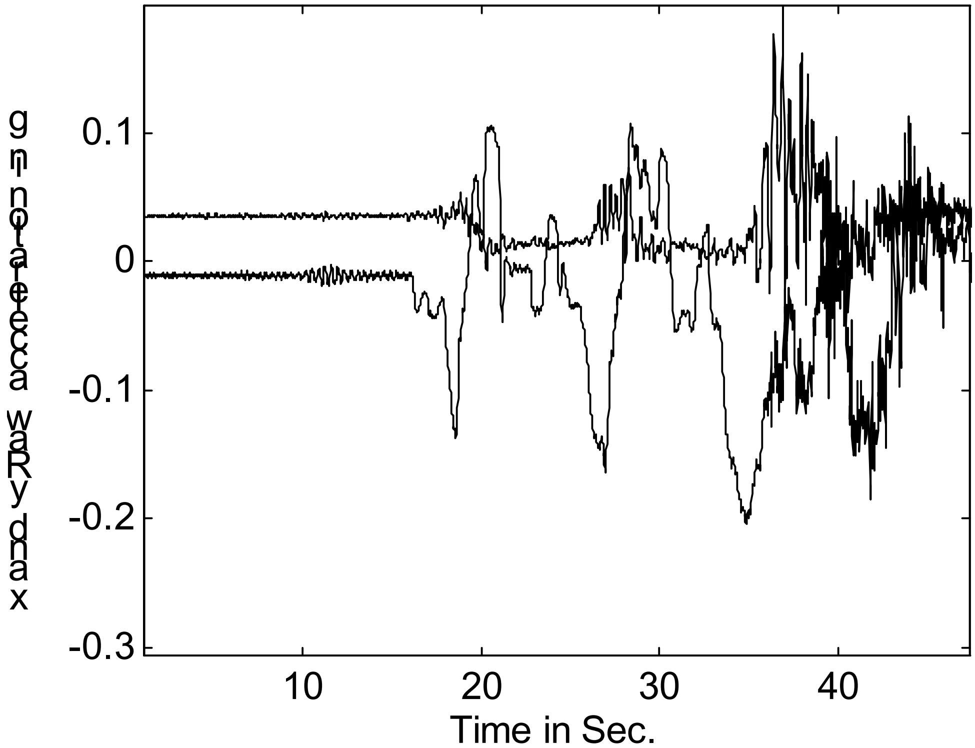

Figure 9. Accelerometers output in body frame

Nebot E., Durrant-Whyte H., "Initial Calibration and Alignment of Low Cost Inertial Navigation Units for Land Vehicle Applications", Journal of Robotics Systems, Vol. 16, No. 2, February 1999, pp. 81-92.

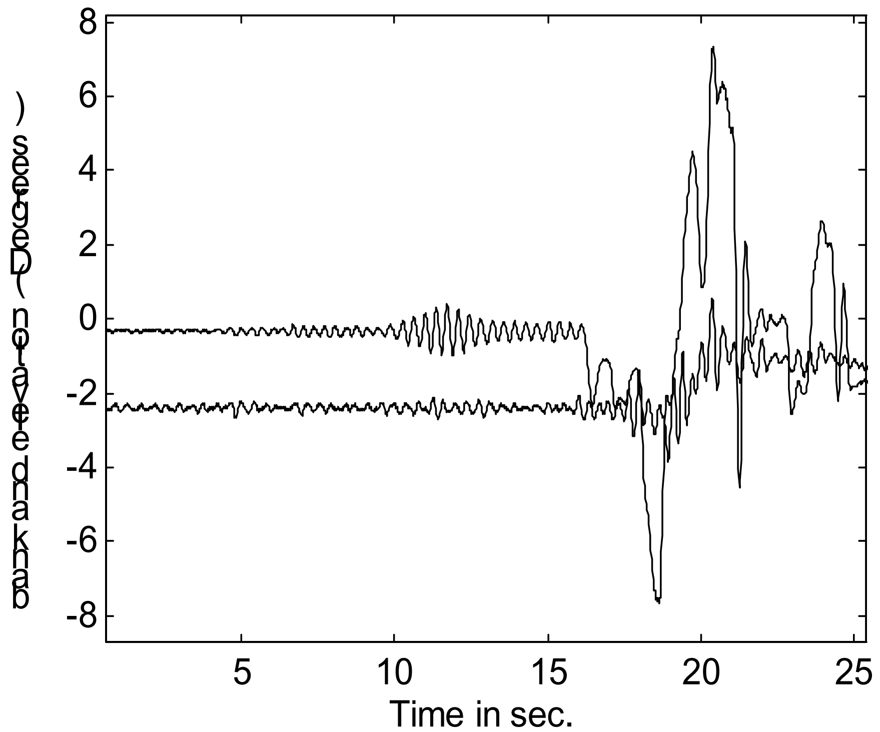

Figure 10. Bank and Elevation output

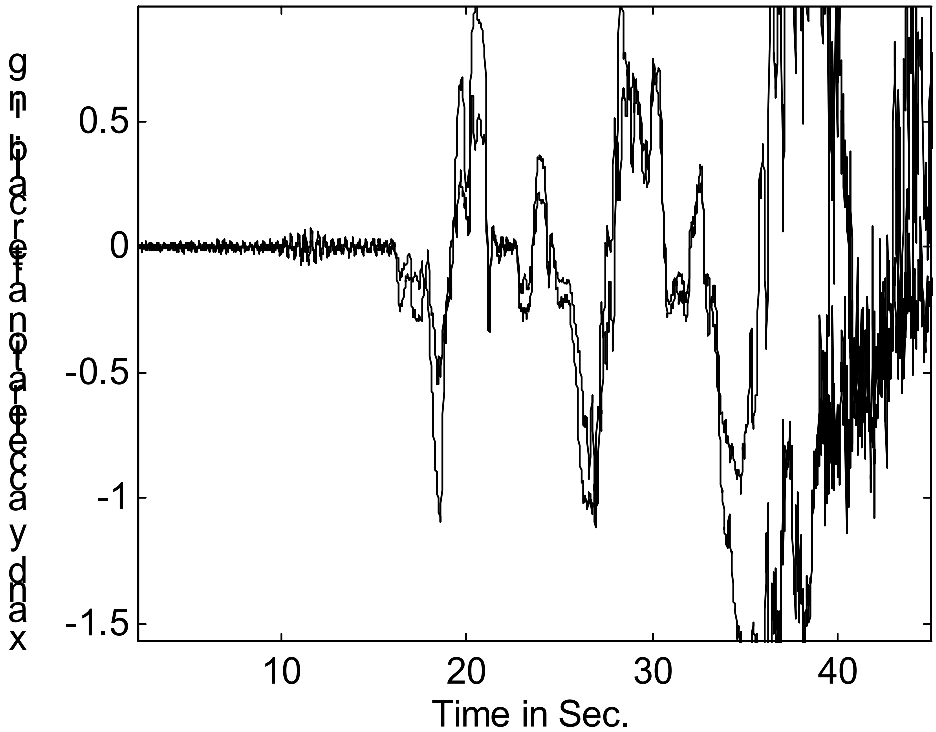

Figure 11. Compensated acceleration (Navigation frame)

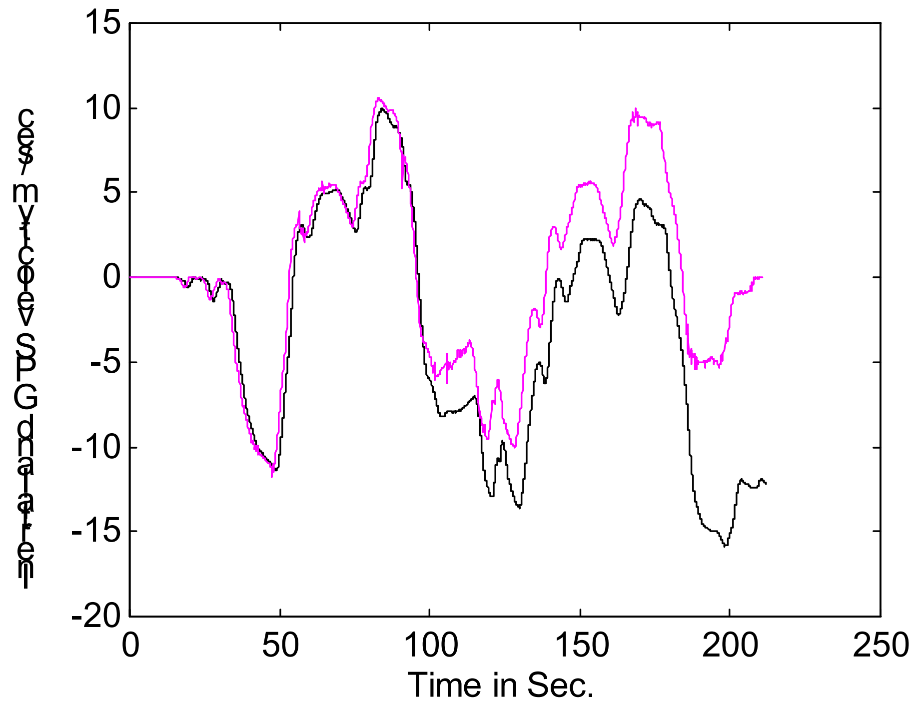

Figure 12. North velocity prediction

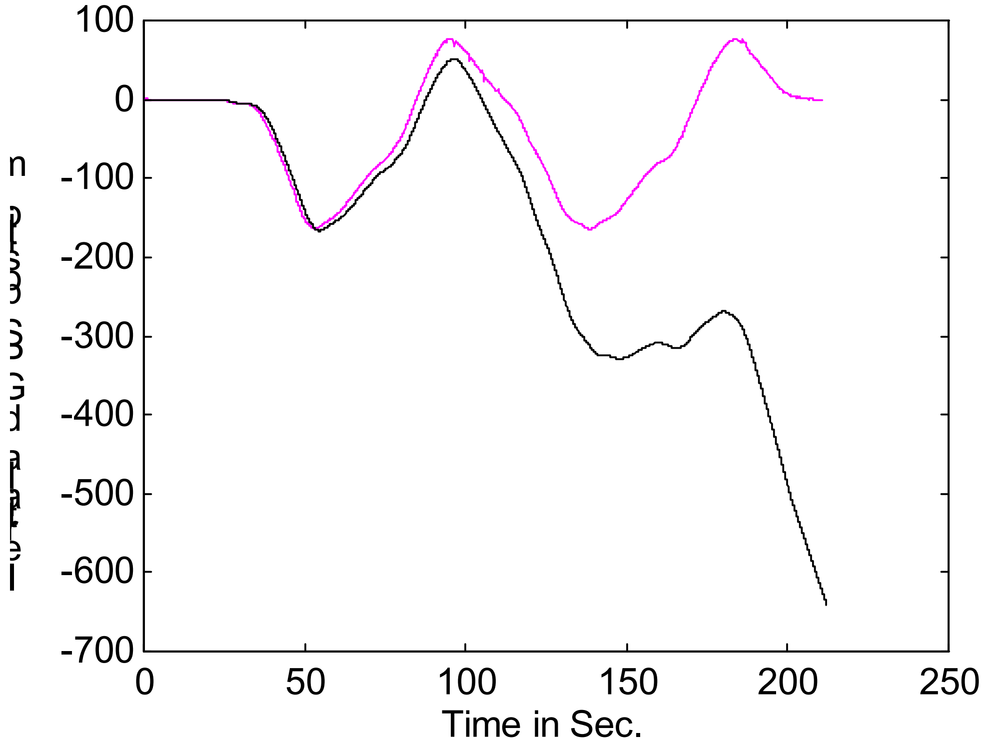

Figure 13. North position prediction

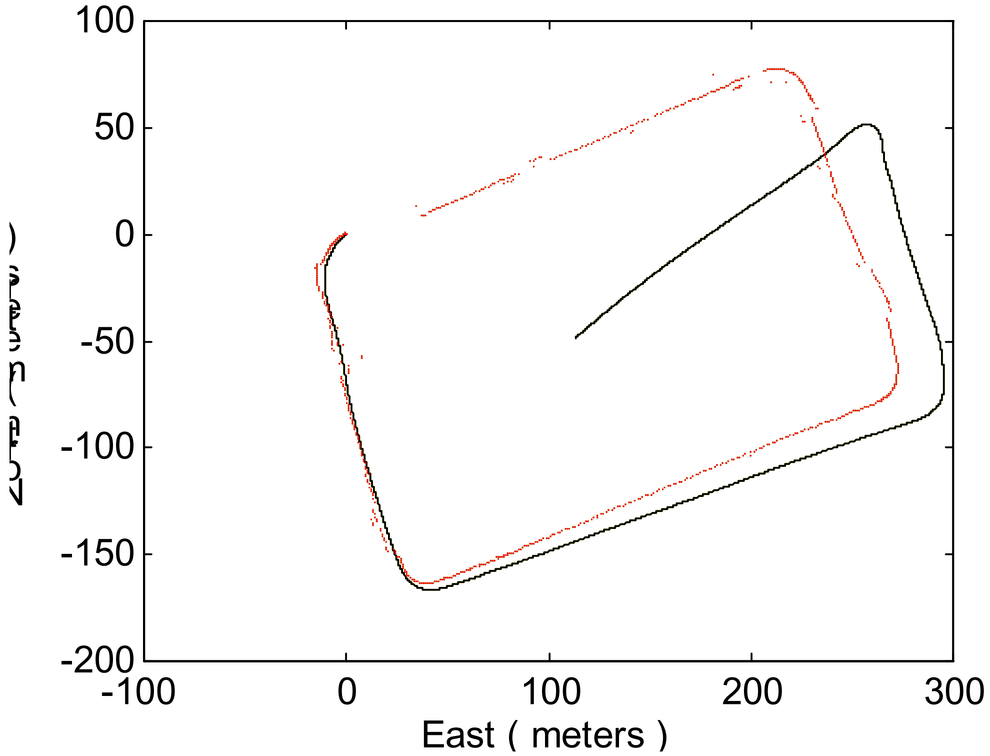

Figure 14. 2-D trajectory prediction

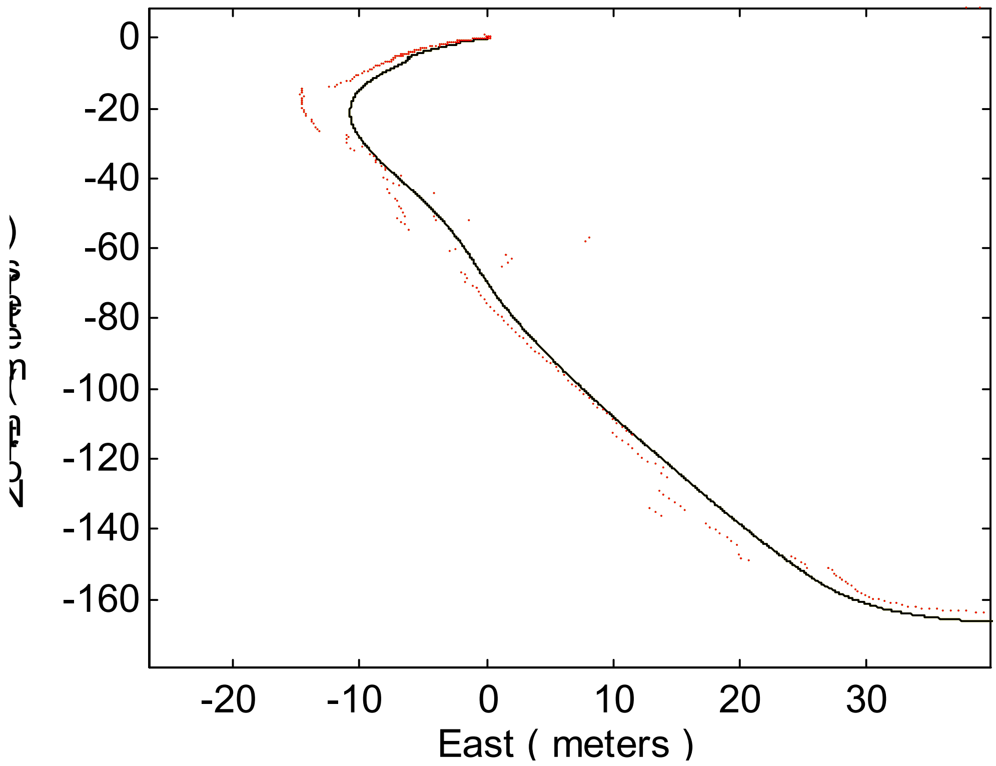

Figure 15. 2-D trajectory prediction

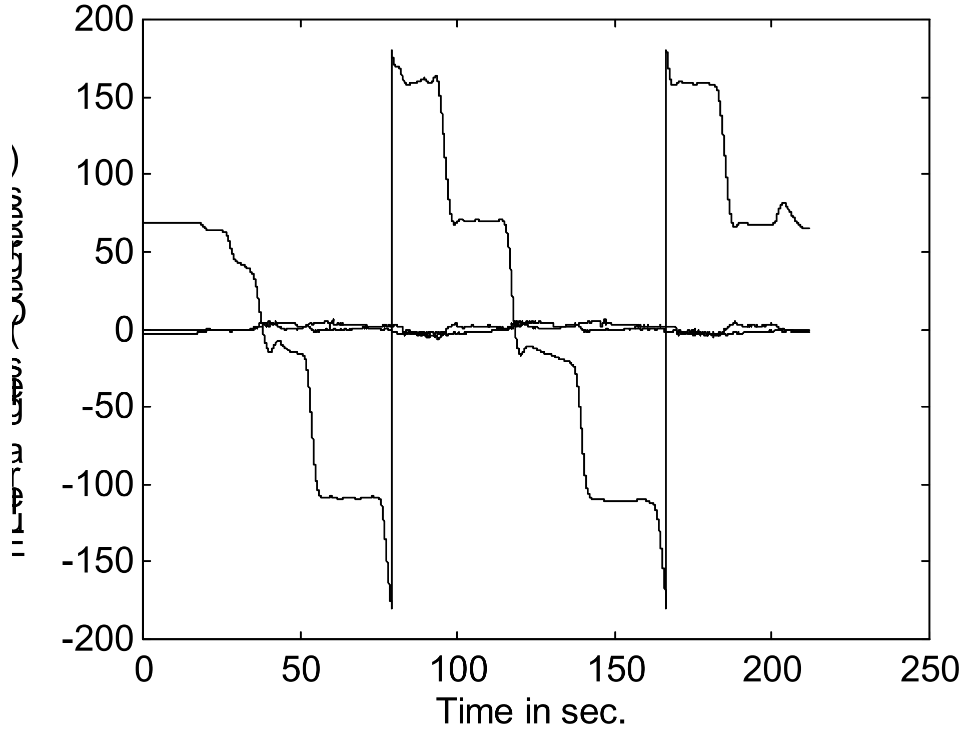

Figure 16. Euler Angles prediction (x,y,z)

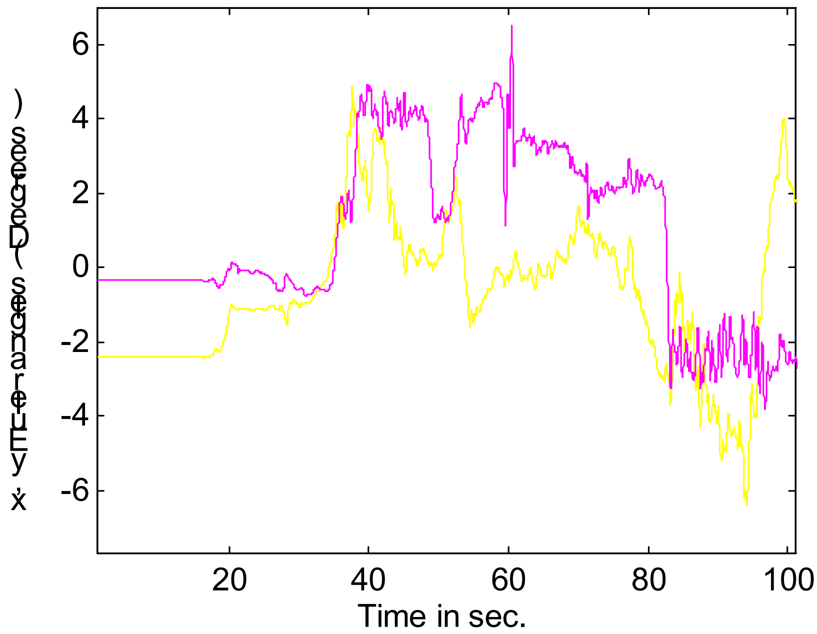

Figure 17. Euler Angles prediction (x,y)